Proceedings of the ASME 2026
International Mechanical Engineering Congress and Exposition
IMECE2026
November 8–12, 2026, Vancouver, British Columbia, Canada

IMECE2026-192934

MULTIFUNCTIONAL LPBF-MANUFACTURED HEAT SINKS WITH INTEGRATED PARTICLE DAMPERS FOR SHOCK MITIGATION IN ELECTRONICS

Digambar Killedar[1], Joud N. Satme[1], Mohsen Zardian[1], Trotter Roberts[1], Patrick Wynne[1], Austin R.J. Downey[1,2,*], Yanzhou Fu[3], and Lang Yuan[1],

[1]Department of Mechanical Engineering, University of South Carolina, Columbia, SC, USA
[2]Department of Civil and Environmental Engineering, University of South Carolina, Columbia, SC, USA
[3]Department of Ocean and Mechanical Engineering, Florida Atlantic University, Boca Raton, FL, USA

ABSTRACT

Laser Powder Bed Fusion (LPBF) enables the fabrication of multifunctional metallic components with integrated internal features that cannot be realized using conventional manufacturing. This study investigates the shock performance of LPBF-manufactured 316L stainless steel heat sinks incorporating internal particle dampers for electronics applications. The heat sink is designed for PCB-mounted systems representative of aerospace electronics operating in high-vibration and high-shock environments. The assembly consists of a printed circuit board configured in a fixed–fixed boundary condition, with the LPBF-manufactured heat sink attached to the MOSFET at the center, providing both thermal management and passive vibration mitigation. Thermal performance is experimentally investigated under controlled heating conditions relative to a baseline solid heat sink. Dynamic performance is evaluated using mechanical shock loading on a drop-table system to replicate harsh environments. Acceleration responses of the PCB–heat sink assembly are measured to assess vibration attenuation and shock response characteristics attributable to the integrated particle damper. It is observed that the particle-damper heat sink reduced the peak acceleration by 6.04% and the second peak by 45.54% compared with the solid heat sink. The combined experimental framework enables evaluation of multi-functional performance under realistic loading conditions. Measured temperature fields, acceleration responses, and observed dynamic characteristics are presented and discussed in the paper to assess the feasibility of LPBF heat sinks with integrated particle dampers for ruggedized electronics applications.

Keywords: Additive manufacturing; Shock and vibration; LPBF; Sensors; FEA; Particle damper

*Corresponding author: austindowney@sc.edu

1. INTRODUCTION

Vibration and temperature controls during operation of electronic assemblies used in aerospace, defense, and other harsh operating environments exposed to combined thermal and dynamic loading are critical [1]. During operation, printed circuit board (PCB) mounted components generate heat while simultaneously experiencing vibration and occasional shock events from launch, flight, transportation, or service conditions. Excessive temperature rise accelerates material degradation and shortens component lifetime. Along with this, uncontrolled vibration can lead to fatigue damage, solder-joint failure [2], loosening of mechanical attachments, and degradation of signal integrity [3].

Electronics packaging for rugged environments requires multi-functional components that can provide both efficient thermal management and passive vibration mitigation within limited space and mass constraints [4]. Laser Powder Bed Fusion (LPBF) additive manufacturing provides a promising solution for developing such multi-functional metallic components [5]. LPBF fabricates parts layer-by-layer, enabling the creation of complex internal cavities, lightweight structures, conformal features, and integrated functional architectures that are difficult or impossible to produce using conventional manufacturing. Previous work by the authors has shown that LPBF can be used for creating geometrically complex features directly inside metallic structures, including internal particle damper cavities that retain unfused powder after printing [6]. These internal powder-filled cavities can act as passive particle dampers without requiring additional external damping hardware, added assembly steps, or dissimilar material inserts [7].

Particle damping is a passive vibration-control mechanism in which mechanical energy is dissipated through repeated particle–particle and particle–wall interactions [6]. The dominant dissipation mechanisms include inelastic collisions, frictional sliding, and momentum exchange between the host structure and the loose granular media. In LPBF-manufactured particle

Copyright ©2026 by ASME

dampers, the retained unfused powder can therefore provide inherent vibration attenuation while preserving the external geometry of the component. This concept is especially attractive for aerospace and electronics applications, where compactness, low added mass, structural integration, and reliability are important design requirements. Prior work on LPBF-integrated particle dampers has demonstrated that unfused powder retained inside internal cavities can significantly reduce vibration response compared with fully solid structures [7]

Although previous studies have focused primarily on structural vibration suppression, relatively limited attention has been given to the combined thermal and dynamic performance of LPBF particle-damper components for electronics [8]. This is an important gap because a heat sink with an internal particle damper must simultaneously satisfy two competing requirements. From a thermal perspective, the component should efficiently conduct heat away from the electronic device and dissipate it through the finned structure. However, introducing an internal cavity and retained powder may alter the heat-transfer path, reduce the effective cross-sectional conduction area, and introduce an equivalent thermal resistance through the powder-filled region [9]. From a vibration perspective, the same cavity can improve energy dissipation if sufficient particle motion is available. Therefore, the design of LPBF heat sinks with internal particle dampers requires understanding both thermal performance and vibration attenuation.

In the present study, an LPBF-manufactured 316L stainless steel heat sink with an integrated internal particle damper is investigated for PCB-mounted electronics applications. The heat sink is mechanically attached to the MOSFET located near the center of a fixed PCB assembly. This configuration is selected to represent practical electronics hardware in which the heat sink must remove heat from the component while also influencing the dynamic response of the PCB assembly under shock excitation. A baseline solid heat sink is used for comparison to evaluate the effect of the internal particle-damper cavity on both heat dissipation and shock vibration response. The thermal performance of the heat sink is experimentally studied under controlled heating conditions. Temperature measurements are used to quantify temperature rise, heat dissipation capability, and thermal resistance relative to the baseline solid heat sink. The vibration performance is evaluated using shock loading. Acceleration responses of the PCB–heat sink assembly are measured to compare the dynamic behavior of the solid and particle-damper heat-sink configurations during these shock or drop events. This enables assessment of the passive vibration-mitigation capability of the integrated powder-filled cavity under transient dynamic excitation.

The main contribution of this study is the experimental evaluation of an LPBF-manufactured multifunctional heat sink that combines thermal management with integrated passive damping. Unlike conventional heat sinks, the proposed design uses an internal particle-filled cavity to provide vibration attenuation while maintaining the primary function of heat dissipation. The combined thermal and shock testing provides an initial assessment of the feasibility of LPBF heat sinks with integrated particle dampers for harsh electronics applications.

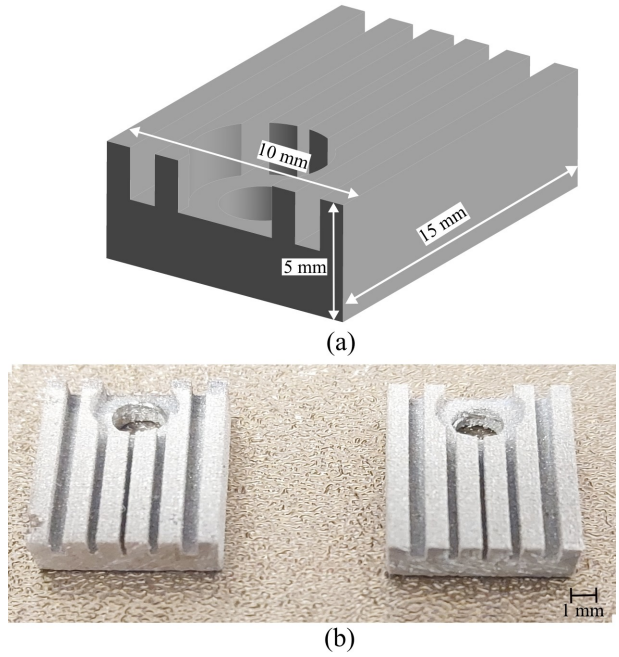


FIGURE 1: Details of damper design, showing: (a) 3D CAD design and; (b) LPBF printed design of particle damper

2. METHODOLOGY

2.1. Experimental Setup

This section describes the experimental framework used to evaluate the multi-functional performance of the LPBF-manufactured heat sink with an integrated particle damper. Figure 1(a) shows the 3D CAD design of the particle damper heat sink, and 3D-printed solid and particle dampers can be seen in Figure 1(b). The methodology consists of two main parts: thermal characterization using infrared imaging and dynamic characterization using shock loading. The test specimen consists of an LPBF-manufactured 316L stainless steel heat sink designed with an internal particle-damper cavity. The parts were fabricated using an Aconity3D MIDI LPBF system under an argon-protected atmosphere. The processing parameters were 150 W laser power, 800 mm/s scan speed, 0.10 mm hatch spacing, and 0.03 mm layer thickness, corresponding to a volumetric energy density of 62.5 J/mm^3. The internal cavity retains unfused powder after fabrication, allowing the heat sink to function as both a thermal-management component and a passive shock-vibration damping element. This design concept follows the general principle of LPBF-integrated particle dampers, where loose powder retained inside internal cavities dissipates mechanical energy through interactions.

For the present study, the heat sink was mechanically attached to the main circuit near the center of a printed circuit board. The PCB was constrained in a fixed–fixed boundary condition to represent a simplified electronics assembly subjected to transient shock or drop-type loading. The chemical composition of the 316L stainless steel used in the LPBF process is shown in Table 1.

Copyright ©2026 by ASME

TABLE 1: Nominal chemical composition of stainless steel 316L, expressed in weight percent (%).

Element	Iron	Ni	Cr	O	Si	S	P	N	C	Mo	Mg	Cu
Weight percent (%)	Bal.	12.7	17.7	0.03	0.62	0.01	0.01	0.10	0.02	2.36	0.65	0.02

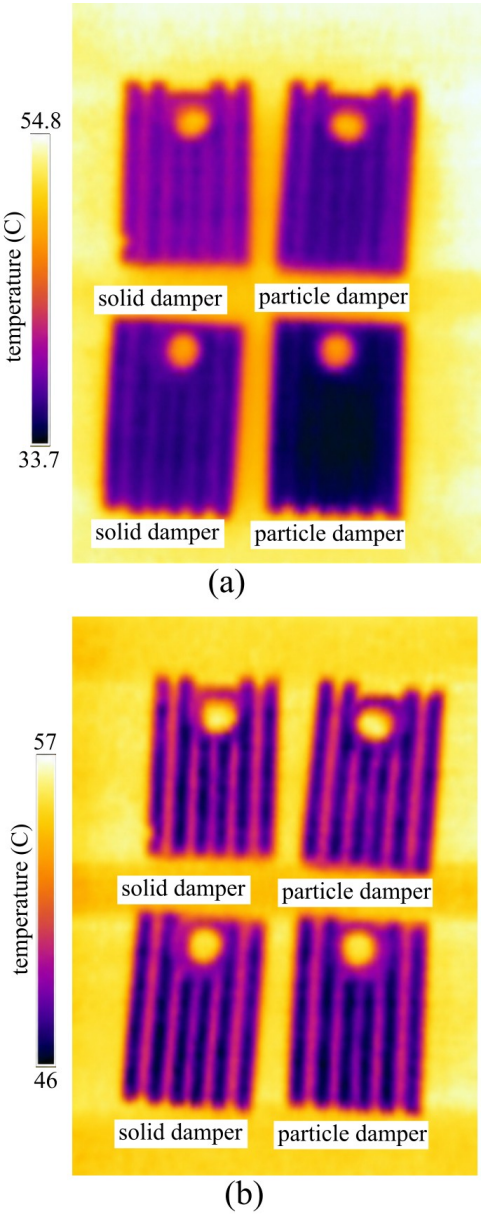


FIGURE 2: Images of solid and particle damper during thermal test, showing: (a) solid and particle damper temperature distribution at time = 1 minute, and (b) solid and particle damper temperature distribution at time = 5 minutes.

2.2. Thermal Testing

Thermal testing was conducted to evaluate the heat-dissipation capability of the LPBF heat sink and to compare the thermal response of the particle-damper heat sink with the baseline solid heat sink. The particle-damper heat sink was placed in a controlled heat bed, which was maintained at 50 degrees

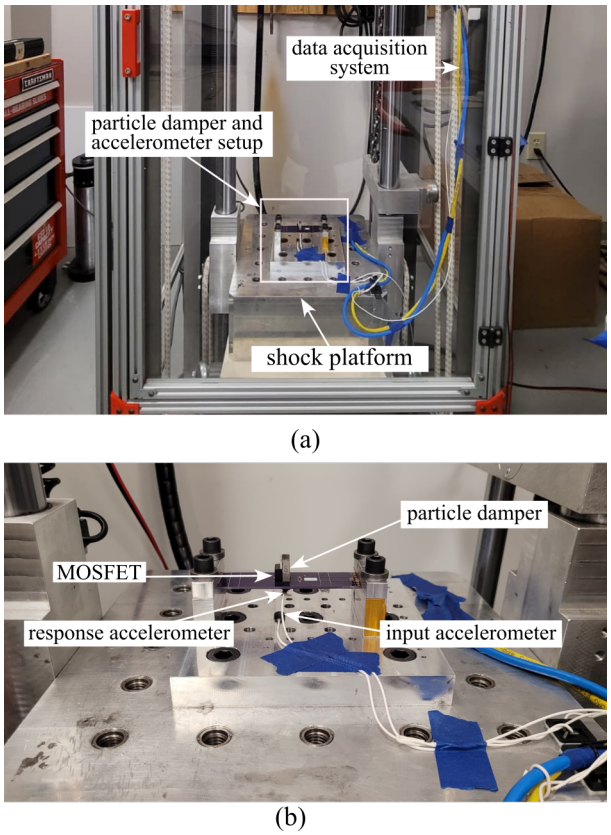


FIGURE 3: Experimental setup for vibration and thermal property testing of particle damper, showing: (a) shock/drop experiment apparatus with data acquisition system; (b) particle damper, MOSFET, and accelerometer setup.

Celsius. A thermal camera was used to capture the transient and steady-state temperature fields of the heat sink, as shown in Figure 2. The camera was positioned to provide a clear view of the heat sink surface and the surrounding region. Thermal images were recorded during heating until the temperature distribution approached steady-state behavior. The same camera position, viewing angle, heating condition, and environmental conditions were maintained for all test cases to ensure a consistent comparison between the solid and particle-damper heat sinks.

2.3. Shock Testing

Shock testing was performed to evaluate the transient dynamic response of the PCB–heat sink assembly under impact or drop-type loading. The experimental setup is shown in Figure 3, which includes the test fixture, data acquisition system, and instrumentation. A close-up view of the PCB assembly is shown in Figure 3(b), where the PCB was mounted in a fixed–fixed boundary condition using a special fixture to reproduce the constraint condition representative of the target electronics application.

Copyright ©2026 by ASME

TABLE 2: Comparison of exponential decay parameters for solid and particle-damper heat sinks under shock excitation.

Metric	Solid	Particle Damper	Improvement
Peak acceleration (g)	182.0	171.0	6.04% ↓
Second peak (g)	59.56	32.43	45.54% ↓
Decay constant, λ	694.7	784.7	12.96% ↑
Estimated damping ratio, ζ	0.151	0.220	46.01% ↑
Settling time to 5% amplitude (s)	0.0043	0.0038	11.47% ↓

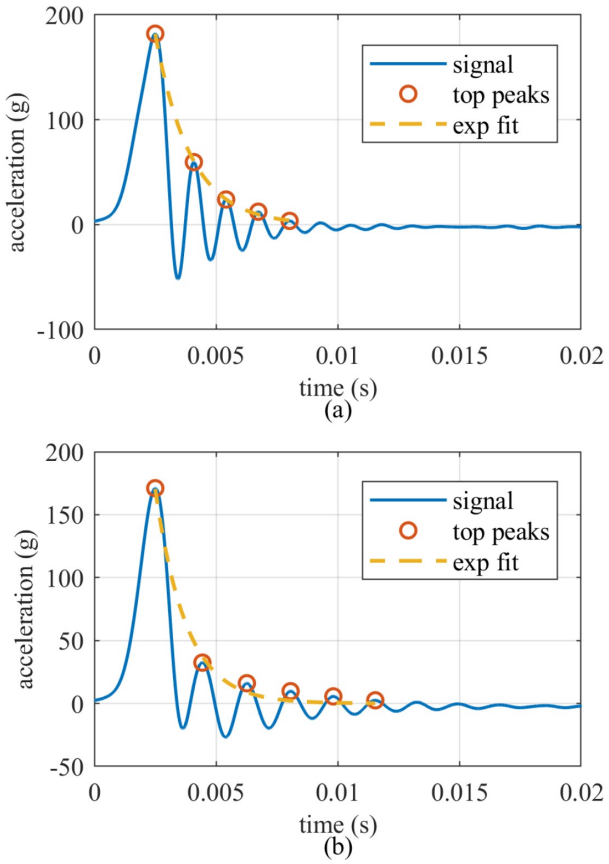


FIGURE 4: Acceleration time histories and exponential decay fits during shock test, showing: (a) solid damper acceleration vs. time under shock test and (b) particle damper acceleration vs. time under shock test.

Shock loading was applied to the assembly, and the acceleration response was recorded for both the baseline solid heat sink and the heat sink with the integrated particle-damper cavity. The measured acceleration time histories were used to compare the transient response of the two configurations after the shock event. Instead of using frequency response functions, the shock response was analyzed in the time domain by examining the decay of acceleration amplitudes and the damping behavior of the PCB–heat sink assembly. The logarithmic decrement was calculated from successive vibration peaks to quantify the damping performance [10]. A faster decay of acceleration amplitude for the particle-damper heat sink was interpreted as evidence of improved shock attenuation due to mechanical energy dissipation inside the internal powder-filled cavity.

3. RESULTS AND DISCUSSION

It is observed from the thermal and shock-vibration test that the LPBF-printed particle damper exhibits both the damping of the vibrations in conjunction with no or minimal effect on the thermal conductivity of the part. This section presents the experimental results obtained from thermal imaging and shock vibration testing of the solid and particle-damper heat sink configurations.

Figure 2(a) and (b) show the thermal response of the solid and particle-damper heat sinks at 1 minute and 5 minutes, respectively. At the end of 1 minute, the particle-damper cavity appears as a cooler region at lower temperatures of around 34 degrees Celsius, indicating a slower temperature rise compared to the surrounding solid material. However, at the end of 5 minutes, both configurations exhibit similar temperature distributions, suggesting that the particle-damper heat sink reaches a comparable steady-state condition. These results indicate that, while the internal cavity affects the transient response, the heat sink still performs its primary thermal function under the tested conditions, though further work is needed to quantify these effects more rigorously.

Figure 4(a) and (b) show the acceleration response of the solid and particle-damper heat sink configurations during shock testing, respectively. The response is plotted in terms of acceleration versus time, and the positive peaks are identified to evaluate the decay and vibration attenuation behavior. An exponential decay fit is included to represent the vibration attenuation trend after the initial shock event.

The damping behavior was quantified using the logarithmic decrement method. For an underdamped free-decay response, the logarithmic decrement was calculated from two vibration peaks as

$$\delta = \frac{1}{n} \ln\left(\frac{x_i}{x_{i+n}}\right),$$

where x_i and x_{i+n} are the amplitudes of two peaks separated by n cycles. The corresponding damping ratio was calculated as

$$\zeta = \frac{\delta}{\sqrt{4\pi^2 + \delta^2}}.$$

In addition, the decay envelope of the acceleration response was fitted using an exponential function,

$$y = Ae^{-\zeta \omega_n t},$$

Copyright ©2026 by ASME

where A is the initial amplitude, ζ is the damping ratio, and ω_n is the natural frequency.

The exponential decay model for the solid heat sink is given by,

$$y = 181.8e^{-694.7t}. \quad (1)$$

The exponential decay model for the particle-damper heat sink is given by

$$y = 170.4e^{-784.7t}. \quad (2)$$

The solid heat sink exhibits a large initial acceleration response followed by several oscillation peaks that decay gradually with time. In comparison, the particle-damper heat sink also shows a strong initial response, but the subsequent vibration amplitudes reduce more rapidly. The peak amplitudes after the first shock pulse are lower for the particle-damper configuration, indicating faster dissipation of the vibration energy. This behavior confirms that the internal particle-filled cavity contributes to passive damping under transient shock excitation. As shown in Table 2, the particle-damper heat sink reduced the peak acceleration by 6.04% and the second peak by 45.54% compared with the solid heat sink. The decay constant increased from 694.7 s^{-1} to 784.7 s^{-1}, while the estimated damping ratio increased by 46.01%. The observed 6.04% reduction in peak acceleration is modest, and it demonstrates that the LPBF-integrated particle dampers can provide measurable passive attenuation without requiring an external damping component. For electronics subjected to repeated shock or drop events, for example, like transportation loads, even moderate reductions in peak acceleration may help reduce transient mechanical loading on solder joints, mounted components, and PCB interfaces. This is a huge improvement, as repeated loading often leads to fatigue failures in these components. Also, further improvement in the damper properties is possible by optimizing powder morphology, packing density, heat-sink geometry, and LPBF printing parameters like laser speed, etc.

4. CONCLUSION

This work presented the feasibility of an LPBF-manufactured multifunctional heat sink with an integrated internal particle damper for PCB-mounted electronics applications. The objective was to evaluate whether the particle-damper heat sink can provide passive vibration mitigation while maintaining thermal performance. Thermal imaging and shock vibration testing were conducted to compare the solid and particle-damper heat sink configurations. Thermal results showed that the solid and particle-damper heat sinks exhibited similar temperature rise and heat distribution under the tested heating conditions. This indicates that the introduction of the internal particle-damper cavity did not significantly affect the heat dissipation capability of the heat sink. Shock vibration results demonstrated that the particle-damper heat sink improved vibration attenuation compared with the solid heat sink. The logarithmic decrement response showed that the vibration amplitudes decayed faster for the particle-damper configuration. This behavior confirms that the retained powder inside the internal cavity dissipates mechanical energy through particle–particle collisions, particle–wall interactions, and frictional sliding. Future work will focus on further quantifying the thermal resistance and vibration environments.

ACKNOWLEDGMENTS

This research was supported by the United States National Science Foundation (NSF), USA, Grants Nos.CCF-2503055, and CPS-2237696. This work is also partially supported by the National Institute of Standards & Technology, United States, under grant number 70NANB23H030, as well as the South Carolina Space Grant Consortium under grants 21-117-RID RGP-SC-009, 25-073-REAP-SC-001, and 25-073-BTC-SC-001. Additional support is provided by the United States' National Science Foundation (NSF) through the NSF ASEE Fellowship. Any opinions, findings, conclusions, or recommendations expressed in this material are those of the authors and do not necessarily reflect the views of the National Science Foundation, the South Carolina Space Grant Consortium, or the National Institute of Standards & Technology.

REFERENCES

[1] Alkhatib, Rabih and Golnaraghi, M. "Active Structural Vibration Control: A Review." *The Shock and Vibration Digest* Vol. 35 No. 5 (2003): pp. 367–383. DOI 10.1177/05831024030355002.

[2] Roberts, Trotter, Burnett, Matthew, Yount, Ryan, Downey, Austin R. J., Moura, Adriane and Abumohaimed, Fahad. "Adaptive shock testing and failure prediction of printed circuit boards using Kriging-based experimental design." Shull, Peter J., Yu, Tzuyang, Gyekenyesi, Andrew L. and Wu, H. Felix (eds.). *Nondestructive Characterization and Monitoring of Advanced Materials, Aerospace, Civil Infrastructure, and Transportation XX*: p. 2. 2026. SPIE. DOI 10.1117/12.3090164.

[3] Steinberg, Dave S. "Vibration analysis for electronic equipment." (2000).

[4] Esser, B. and Huston, D. "Active mass damping of electronic circuit boards." *Journal of Sound and Vibration* Vol. 277 No. 1-2 (2004): pp. 419–428. DOI 10.1016/j.jsv.2003.11.055.

[5] Chowdhury, Sohini, Yadaiah, N., Prakash, Chander, Ramakrishna, Seeram, Dixit, Saurav, Gupta, Lovi Raj and Buddhi, Dharam. "Laser powder bed fusion: a state-of-the-art review of the technology, materials, properties & defects, and numerical modelling." *Journal of Materials Research and Technology* Vol. 20 (2022): pp. 2109–2172. DOI 10.1016/j.jmrt.2022.07.121.

[6] Satme, Joud, Fu, Yanzhou, Roberts, Samuel, Downey, Austin, Tianyu, Zhang, Yuan, Lang and Kiracofe, Daniel. "Tunable shock and vibration damping in metal laser powder bed fusion components via controlled post-print compaction of particle damper cavities." *Smart Materials and Structures* Vol. 35 (2026). DOI 10.1088/1361-665X/ae59d7.

[7] Ehlers, Tobias, Oel, Marcus, Tatzko, Sebastian, Kleyman, Gleb, Niedermeyer, Jens, Wallaschek, Jörg and Lachmayer, Roland. "Design Guidelines for Additive Manufactured Particle Dampers: A Review." *Procedia CIRP* Vol. 119 (2023): pp. 891–896. DOI 10.1016/j.procir.2023.03.134.

[8] Scott-Emuakpor, Onome, Beck, Joseph, Runyon, Brian, Holycross, Casey, Sheridan, Luke, O'Hara, Ryan and George, Tommy. "Determining unfused powder threshold

Copyright ©2026 by ASME

for optimal inherent damping with additive manufacturing." *Additive Manufacturing* Vol. 38 (2021): p. 101739. DOI 10.1016/j.addma.2020.101739.

[9] Simmons, Jacob C., Chen, Xiaobo, Azizi, Arad, Daeumer, Matthias A., Zavalij, Peter Y., Zhou, Guangwen and Schiffres, Scott N. "Influence of processing and microstructure on the local and bulk thermal conductivity of selective laser melted 316L stainless steel." *Additive Manufacturing* Vol. 32 (2020): p. 100996. DOI https://doi.org/10.1016/j.addma.2019.100996. URL https://www.sciencedirect.com/science/article/pii/S2214860419314381.

[10] Downey, Austin and Micheli, Laura. "Vibration Mechanics: A Practical Introduction for Mechanical, Civil, and Aerospace Engineers." (2026)DOI 10.31224/6182.

Copyright ©2026 by ASME